

Leaky Dams

Rob Gondris

21 September 2020

1 Summary

In this project, I investigate the effectiveness of Leaky Dams for flood prevention, specifically for large catchments. I model the potential effectiveness of these Leaky Dams, and compare it to the results found for smaller catchment sizes.

This project extends the ideas presented in Hankin et al [1]. I first derive a system of ordinary differential equations that model river flow, where one dam can be placed in each segment. I then write code that gives a numerical solution. I apply this to a large catchment in Cumbria, UK. I investigate the results and show how dam design affects performance, and highlight the benefits of using a model to specify dam design.

2 Introduction

There is a growing interest in ‘Leaky Dams’, a low cost nature-based flood barriers. These are intended to be located on upstream branches in a river catchment. They are part of the UK Government’s plan for working with natural processes to reduce flood risk (Environment Agency, [2]), and are often contained in nature based approaches to flood prevention (Nicholson [3]).

Leaky dams are designed to simulate fallen trees and often built to be permeable. This means that they have little affect on the stream if the flow through it is small, however they hold back more water as the flow through it increases. An example is shown in Figure 1. They are currently seen by the UK government as an additional prevention measure, and not as a replacement for traditional flood prevention strategy (GOV.UK [4]). In this project, I modify the approach taken in Hankin et al [1]. I model the river as a series of uniform segments, and derive a system of differential equations to model how the flow evolves. I write code to solve this numerically in Python and explain the code with worked examples. I also give various methods of visualising the results. The code is presented in Jupyter notebooks in GitHub¹.

The model is then applied to a large catchment, the source of the river Kent in Cumbria, Britain. The Kent is prone to flooding, for example during storm Ciara in February 2020 (BBC [9]). I model what effect different dam set-ups have, and how the design of the dams influence their effectiveness.

¹<https://github.com/robgondris/network-flood-model>



Figure 1: Leaky dam near Reston, Scotland. Jayne Wilkinson (South Cumbria Rivers Trust)

3 Derivations

3.1 Overview

A river network is modelled as a set of idealised segments, where flow is uniform within each segment. A key property of a leaky dam is that it should not have a large impact on a segment if there isn't much water flowing through it. I use a simple model for a dam, by allowing the base of the dam to be a set height above the segment base. The following model is an extension of the one in Hankin, Hewitt [1]. I use two different methods for solving the system of differential equations and compare the two. A mathematically derived model is necessary because there is a lack of empirical data for leaky dams (

3.2 Set-up

The river network is modelled as a collection of N river segments. Label these R_i , where i ranges from 1 to N . Construct a directed graph $G = (R, \vec{E})$, where R is its vertex set and \vec{E} is its edge set. The vertices of G correspond to river segments, so $R = \{R_i : i = 1, \dots, N\}$. G has a directed edge $\{R_i R_j\} \in \vec{E}$ if segment R_i flows directly into segment R_j . See Figure 2 for an example.

For computational simplicity, segments are modelled as rectangular with widths w_i , slopes S_i , and lengths l_i . Here $S_i = \tan(\theta_i)$ where θ_i is the angle the river bed makes with the horizontal. An important property of a leaky dam is that it has minimal impact when the flow is small. To get this behaviour, I closely follow the method in Hankin, Hewitt [1], where dams are H_u m tall but have a gap of height H_l m under which water flows without restriction. The variable h measures the height of water at the dam, and the variable h_{stream} measures the height of water downstream from the dam. See Figure 3 for a diagram. Table 17 is a summary of all of the variables used in this section.

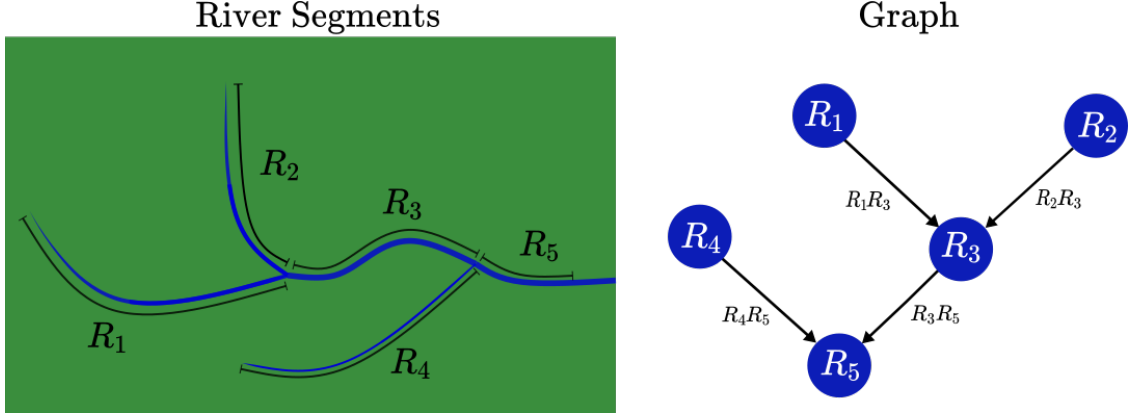


Figure 2: Example river network and corresponding directed graph.

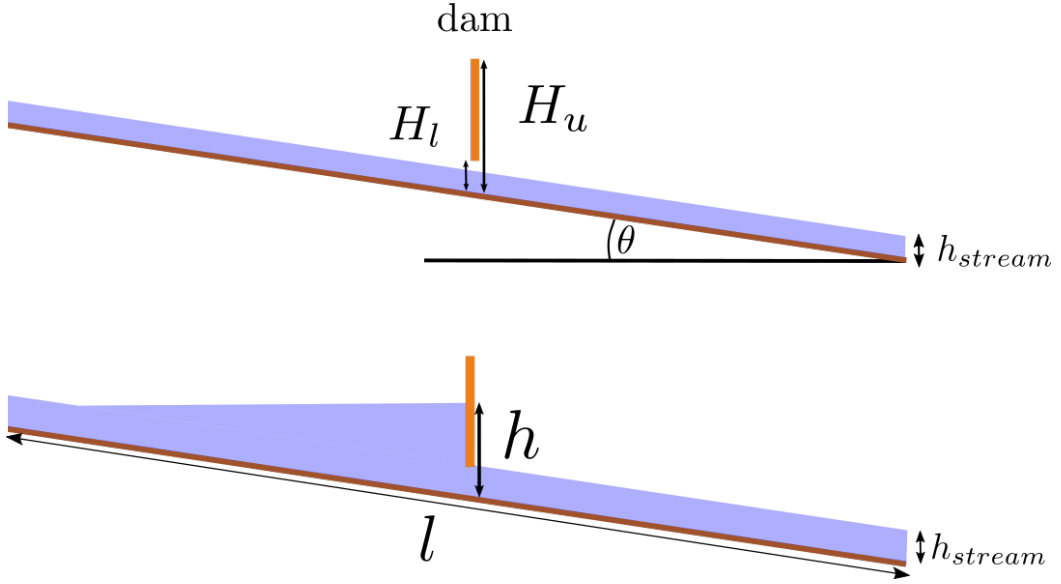


Figure 3: Segment cross-section with dam for two different flows

3.3 Governing Equations

For each river segment R_i , define V_i as the total volume of water it contains and Q_i as the flow leaving it. Let $q_i(t)$ be the inflow into R_i at time t - this models inflow from rain and groundwater, and in applications will have to be measured or modelled using over-land rain models, for example see Metcalfe, Bevan, Hankin [5]. Conservation of mass gives the differential equation

$$\frac{dV_i}{dt} = \sum_{\substack{j \\ \{R_j R_i\} \in E}} Q_j - Q_i + q_i(t)$$

for each segment. This system can then be written as

$$\frac{d\mathbf{V}}{dt} = A^\top \mathbf{Q} - \mathbf{Q} + \mathbf{q}(t) \quad (4)$$

where $\mathbf{V} = (V_1, \dots, V_N)$, $\mathbf{Q} = (Q_1, \dots, Q_N)$, $\mathbf{q}(t) = (q_1(t), \dots, q_N(t))$, and A is the adjacency matrix of the graph G .

In order to solve this, \mathbf{Q} and \mathbf{V} need to be related. Q_i can be calculated as a function of h_i with widely used empirical formulae. First, finding calculating the flow Q . Note the subscripts i have been dropped for simplicity - all of the following equations in this section are for a single segment. The following formulae are from Munson et al [6].

Free flow in a rectangular channel with hydraulic radius r_h is given by

$$Q = \frac{1}{n} w h r_h^{2/3} \sqrt{S}, \quad r_h = \frac{wh}{w + 2h}.$$

This is an empirical formula that involves the Manning coefficient n - a measure of how 'rough' part of a river is. A discussion on finding the correct values for a given application can be found in Chow, 1985 [7]. A simplification to this formula is to make a hydraulic assumption that h will be small compared to w , so $w + 2h \approx w$ (Hewitt, I [8]). Under this assumption, the relation is

$$Q = \frac{1}{n} w h^{5/3} \sqrt{S}. \quad (5)$$

Flow under a sluice gate is given by Bernoulli's equation

$$Q = w \sqrt{2g} \frac{h H^l}{\sqrt{h + H^l}} \quad (6)$$

where H^l is the distance between the channel bottom and the bottom of the sluice and $g \approx 9.8$ is acceleration due to gravity

Flow over a weir is given by

$$Q = C_{wr} \frac{2}{3} \sqrt{2g} w \max(0, h - H^u)^{3/2} \quad (7)$$

where H^u is the weir height and h is the downstream height. C_{wr} is the weir coefficient, taken here to be 0.6 (Munson et al [6]).

Since the dams being modelled are leaky, they should also be at least somewhat permeable. This could be achieved with a permeability term of the form

$$Q = k w \sqrt{2gh} \min(h - H_l, H_u - H_l) . \quad (8)$$

This depends on a non dimensional permeability constant k . Since there is a lack of data to compute a reasonable value for this, $k = 0$ from here on. It is however kept for completeness.

Consider these relations as functions for Q in terms of river height at the dam h . From above, there are two different predictions for flow through the leaky dam. Friction limited flow:

$$Q_{fric}(h) = \frac{1}{n} w h^{5/3} \sqrt{S} \quad (9)$$

and dam limited flow:

$$Q_{dam}(h) = w \sqrt{2g} \left[\frac{H^l h}{\sqrt{h + H^l}} + k \sqrt{h} \min(h - H^l, H^u - H^l) + \frac{2}{3} \max(0, h - H^u)^{3/2} \right] . \quad (10)$$

Dam limited flow is found as the sum of Equations 6, 7 and 8.

Also note that the dam can only limit the flow if $h \geq H^l$. This means that care needs to be taken when deciding which flow value to use. Note in general $Q_{fric}(H^l) \neq Q_{dam}(H^l)$. This is expected, as the formulae come from different empirical sources. However, this is also consistent theoretically as the base of the dam will impact stream flow due to viscosity.

- If $Q_{fric}(H_l) \geq Q_{dam}(H_l)$ then the dam immediately assumes hydraulic control. Note it is sensible to allow the flow Q to be able to decrease here.
- If $Q_{fric}(H_l) < Q_{dam}(H_l)$ then the flow is still friction limited, and the dam has yet to impact flow. There will be a critical value h_{crit} (where $h_c \geq H_l$) satisfying $Q_{fric}(h_c) = Q_{dam}(h_c)$.²

Defining a critical switching height h_{crit} for both cases:

$$h_{crit} = \begin{cases} H_l & Q_{fric}(H_l) \geq Q_{dam}(H_l) \\ h_c & Q_{fric}(H_l) < Q_{dam}(H_l) \end{cases}$$

Define the flow through a dam given the height of water behind it h as:

$$Q^*(h) = \begin{cases} Q_{fric}(h) & h < h_{crit} \\ Q_{dam}(h) & h \geq h_{crit} \end{cases} \quad (11)$$

Note $Q^*(h)$ is a function whereas Q is the theoretical flow out of a segment, so Q^* and Q are not interchangeable.

The volume of water in a segment is given by:

$$V^*(h; h_{stream}) = \begin{cases} wlh_{stream} + \frac{w}{2S} \max(0, h - h_{stream})^2 & h < h_{stream} + Sl \\ wl(h - \frac{1}{2}Sl) & h \geq h_{stream} + Sl \end{cases}$$

where h_{stream} is the height of the free flowing water in the segment. The first case is where the reservoir doesn't take up the length of the segment, and the second if the water has backed up behind the dam enough to fill the whole segment. See Figure 3 shows the dam set-up.

However, given examples of existing dams, this would underestimate the volume of water that can be stored behind a dam. This is due to the dam causing the stream to back up and burst its banks. To address this, I add a storage coefficient $\lambda \geq 1$ which increases the volume of water that a dam can store. $V^*(h)$ is then

$$V^*(h; h_{stream}) = \begin{cases} wlh_{stream} + \lambda \frac{w}{2S} \max(0, h - h_{stream})^2 & h < h_{stream} + Sl \\ wlh_{stream} + \frac{\lambda}{2} wSl^2 + wl(h - h_{stream} - Sl) & h \geq h_{stream} + Sl \end{cases}$$

² $Q_{fric}(h) = \mathcal{O}(h^{5/3})$ whereas $Q_{dam}(h) = \mathcal{O}(h^{3/2})$

which is equivalent to

$$V^*(h; h_{stream}) = \begin{cases} wlh_{stream} + \lambda \frac{w}{2S} \max(0, h - h_{stream})^2 & h < h_{stream} + Sl \\ wl\left(h - (1 - \frac{\lambda}{2})Sl\right) & h \geq h_{stream} + Sl \end{cases}. \quad (12)$$

To use this, h_{stream} needs to be found. Inverting Equation 5 and assuming $Q = Q^*(h)$ gives

$$h_{stream}(h) = \left(\frac{nQ^*(h)}{w\sqrt{S}}\right)^{3/5}. \quad (13)$$

Taking $V^*(h) = V^*(h, h_{stream}(h))$ makes V a function of h only.

3.4 Nondimensionalisation

The variables w , l , h , S , Q , V , t will be nondimensionalised. Dimensionless constants α and β are also defined. The constants are denoted with a subscript c (e.g. V_c) and the nondimensional variables with hats (e.g. \hat{V}).

$$t = t_c \hat{t} \quad l = l_c \hat{l} \quad w = w_c \hat{w} \quad h = h_c \hat{h} \quad S = S_c \hat{S} \quad V = V_c \hat{V} \quad Q = Q_c \hat{Q}$$

To determine the correct nondimensional constants, l_c , w_c , h_c and S_c should be taken to correspond roughly to their average values for a specific problem. Then define

$$Q_c = w_c h_c^{3/5} \sqrt{S_c}, \quad t_c = \frac{l_c w_c h_c}{Q_c}, \quad V_c = l_c w_c h_c, \quad \alpha = \frac{w_c h_c^{3/2} \sqrt{2g}}{Q_c}, \quad \beta = \frac{h_c}{l_c S_c}.$$

The problem now becomes:

$$\frac{d\hat{V}}{d\hat{t}} = A^\top \hat{Q} - \hat{Q} + \hat{q}(\hat{t}) \quad (14)$$

$$\hat{Q}^*(h) = \begin{cases} \frac{1}{n} wh^{5/3} \sqrt{S} & h < \hat{h}_{crit} \\ \alpha w \left[\frac{H^l h}{\sqrt{h + H_l}} + 0.6 \cdot \frac{2}{3} \max(0, h - H^u)^{3/2} \right] & h \geq \hat{h}_{crit} \end{cases} \quad (15)$$

$$\hat{V}^*(h) = \begin{cases} \hat{w}\hat{l}\hat{h}_{stream} + \frac{1}{\beta} \lambda \frac{\hat{w}}{2\hat{S}} \max(0, h - \hat{h}_{stream})^2 & h < \hat{h}_{stream} + \beta \hat{S}\hat{l} \\ \hat{w}\hat{l}\left(h - \beta(1 - \frac{\lambda}{2})\hat{S}\hat{l}\right) & h \geq \hat{h}_{stream} + \beta \hat{S}\hat{l} \end{cases}. \quad (16)$$

$$\text{Where } \hat{h}_{stream} = \left(\frac{n\hat{Q}^*(h)}{\hat{w}\sqrt{\hat{S}}}\right)^{3/5}.$$

3.5 Notation

A summary of notation used, all of the below are given for segment R_i and are the non-dimensional versions. Vector versions are also defined to simplify notation.

l_i	Length	H_i^l	Lower dam height
w_i	Width	H_i^u	Upper dam height
S_i	Slope	k_i	Dam permeability
h_i	River height at dam	λ_i	Dam storage coefficient
n_i	Manning (roughness) coefficient	$h_{\text{stream}}(h)$	Downstream height function
V_i	Volume of water in segment	$Q_i^*(h)$	Flow function
$q_i(t)$	Inflow at time t	$V_i^*(h)$	Volume function
A	Adjacency matrix of G		
\mathbf{V}	$(V_1, V_2, \dots, V_N)^\top$		
\mathbf{Q}	$(Q_1, Q_2, \dots, Q_N)^\top$		
\mathbf{h}	$(h_1, \dots, h_N)^\top$		
$\mathbf{V}^*(\mathbf{h})$	$(V_1^*(h_1), \dots, V_N^*(h_N))^\top$		
$\mathbf{Q}^*(\mathbf{h})$	$(Q_1^*(h_1), \dots, Q_N^*(h_N))^\top$		
$\mathbf{q}(t)$	$(q_1(t), \dots, q_N(t))^\top$		

Table 17: Notation

3.6 Computational Approaches

There are different possible methods to solve the system of ODEs (number). The system is a differential equation for $\mathbf{V}(t)$. One approach is to try and express \mathbf{Q} as a function of \mathbf{V} , for example by finding an inverse to $\mathbf{V}^*(\mathbf{h})$ (say $\mathbf{f}(\mathbf{V})$) and setting $\mathbf{Q} = \mathbf{Q}^*(\mathbf{f}(\mathbf{V}))$. However, Q is not necessarily monotone increasing, and V depends on Q via h_{stream} . A monotone approximation can be used, which although it is computationally efficient, may lose accuracy especially if $h_i \approx H_i^l$ for some i .

A potential issue with this method is that differential equations can lead to hysteresis - this is the dependence of a solution on its previous states. This comes from the potential non-monotonicity of $Q^*(h)$, as there may be multiple solutions to $Q^*(x) = Q_0$ if Q_0 is chosen appropriately.

An approach which satisfies this is to also solve for \mathbf{h} . To do this, we need to add a differential equation for \mathbf{h} . The following system of $2N$ variables will give the correct behaviour, where $\varepsilon \geq 0$ is a small constant:

$$\varepsilon \frac{d\hat{\mathbf{h}}}{d\hat{t}} = \hat{\mathbf{V}} - \hat{\mathbf{V}}^*(\hat{\mathbf{h}}) \quad (18)$$

$$\frac{d\hat{\mathbf{V}}}{d\hat{t}} = A^\top \hat{\mathbf{Q}}^*(\hat{\mathbf{h}}) - \hat{\mathbf{Q}}^*(\hat{\mathbf{h}}) + \hat{\mathbf{q}}(\hat{t}) \quad (19)$$

This needs some explanation. Note that the difference between $\hat{\mathbf{V}}$ and $\hat{\mathbf{V}}^*(\hat{\mathbf{h}})$ is critical here. Both equations are defined on the nondimensionalised variables. Because of this, taking ε to be small makes $\hat{\mathbf{h}}$ evolve on a faster timescale than $\hat{\mathbf{V}}$. For a fixed $\hat{\mathbf{V}}$, the stationary points of Equation 18 are values \mathbf{y} satisfying $\hat{\mathbf{V}} = \hat{\mathbf{V}}^*(\mathbf{y})$.

The specific value should be chosen once the nondimensionalisation constants are set to make sure \mathbf{h} evolves on a faster timescale than \mathbf{V} . Note that this sidesteps the problem of inverting $\hat{\mathbf{V}}^*(\hat{\mathbf{h}})$, and deals with the potential non-monotonicity of $\hat{\mathbf{Q}}^*(\hat{\mathbf{h}})$. A large disadvantage of this method is that equations (18), (19) have \mathbf{h} and \mathbf{V} vary on different timescales. This is a typical example of a stiff numerical problem - which will decrease the efficiency of a numerical solver.

3.7 Comparing Approaches

This section will be a comparison of the two above approaches. The code for these, as well as the code and data for the application, are available on GitHub³. This contains notebooks working through the implementation with example results. The plots below are using this code.

I will compare models on a toy network consisting of four segments in a line, that is $G = (\{R_1, R_2, R_3, R_4\}, \{R_1R_2, R_2R_3, R_3R_4\})$. These have $l = 100, w = 2, S = 0.05$ and $\lambda = 10$, which represent a typical small river segment. The inflow is Gaussian into the first segment only, this would model an intermediate part of a river network. Here, $H^u = 1.5$ and H^l varies. See Figure 20.

There are small differences in the height plots, but methods give the same flow results. Flow is the more important result here. However, there are some situations where the models predict different results, where the numerical approximation doesn't capture the hysteresis of the problem. An example is shown in Figure 21. This uses the same parameters as above, with $H^l = 0.2$, but a different rain inflow. In this, the hysteresis model allows for two different steady states for h which give the same flow value. Note however that both models give the same flow results.

The plots in Figure 20 show the importance of determining a good value for H^l . If it is too low, for example Figure 20 a), then the dams will have already been filled up before the worst of the flood has reached them. This means that there will be minimal impact on the maximum flow value. However if H^l is too high, then it might not have any impact at all - if for example the river segment height never reaches it.

For networks modelling small catchments, so with small flow values, this situation is less of an issue as the total volume that a dam set-up can store will be of a similar order to the total volume of water that flows through the network during the course of a flood. However, when designing a dam set-up for a larger network care needs to be taken to ensure the dams only impact near the peak of a flood. This is illustrated in Section 4.4.

³<https://github.com/robgondris/network-flood-model>

Flow and Height plots for R_4

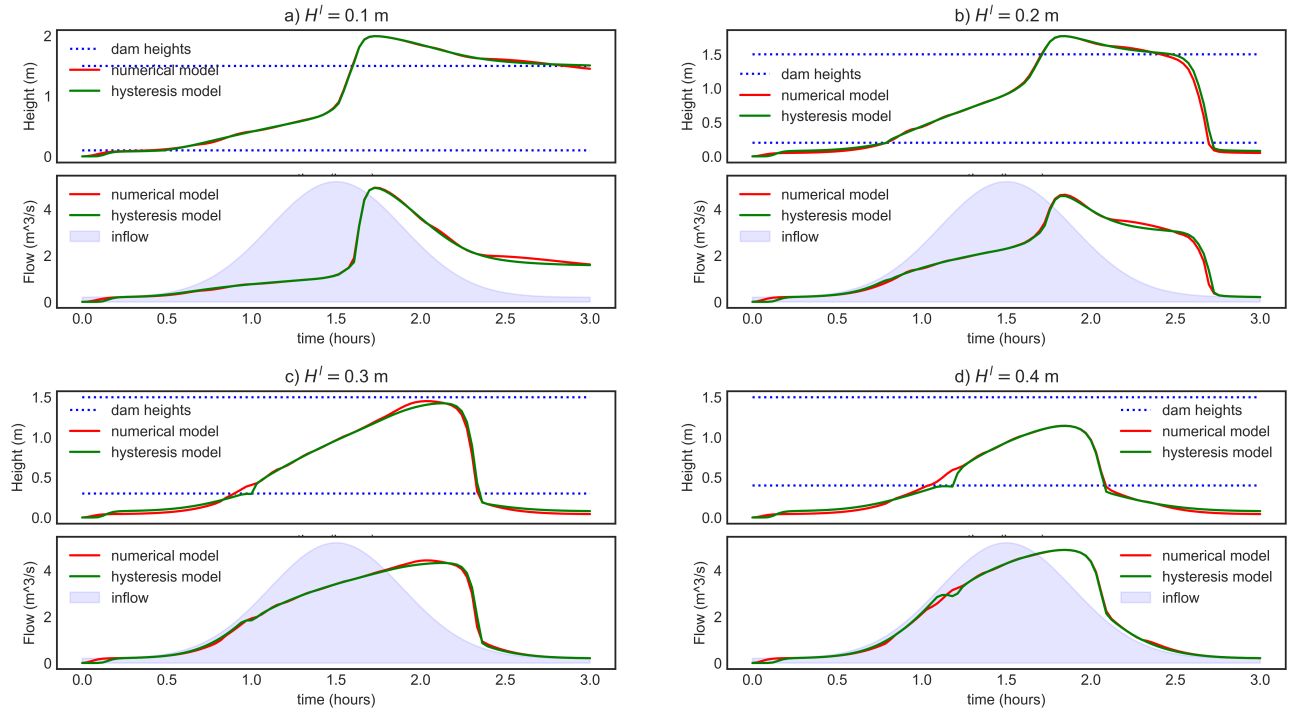


Figure 20: Comparing Methods, segment details given in 3.7

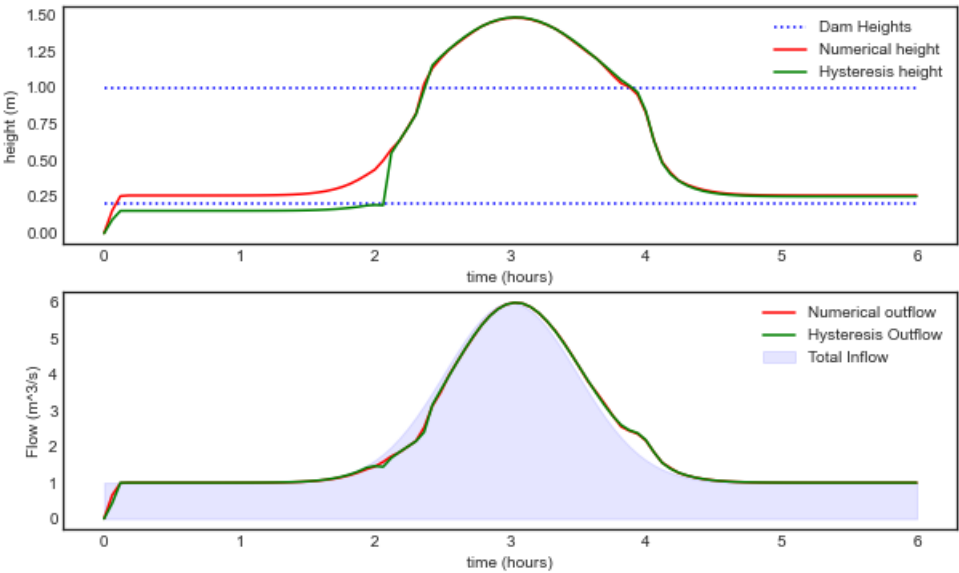


Figure 21: Dam plot for $H^l = 0.22$, segments as in Figure 20

4 Application

In this section, I apply the model to a large network to assess the potential effectiveness of building dams here. The location was suggested by Barry Hankin, who also kindly provided data on the network and a rainfall profile.

The river network is the catchment to Bowston in Cumbria, England. See Figure 22. This catchment is the source of the river Kent, with a catchment area of 70.6 km^2 . The river Kent is prone to flooding downstream, for example Kendal during storm Ciara in early February 2020.(BBC news, 2020 [9]). The South Cumbria Rivers Trust will start implementing Natural Flood Measures (of which Leaky Dams are a part of) as part of a DEFRA funded scheme to mitigate flooding [11], here I will assess the potential effectiveness of a dams near the source.

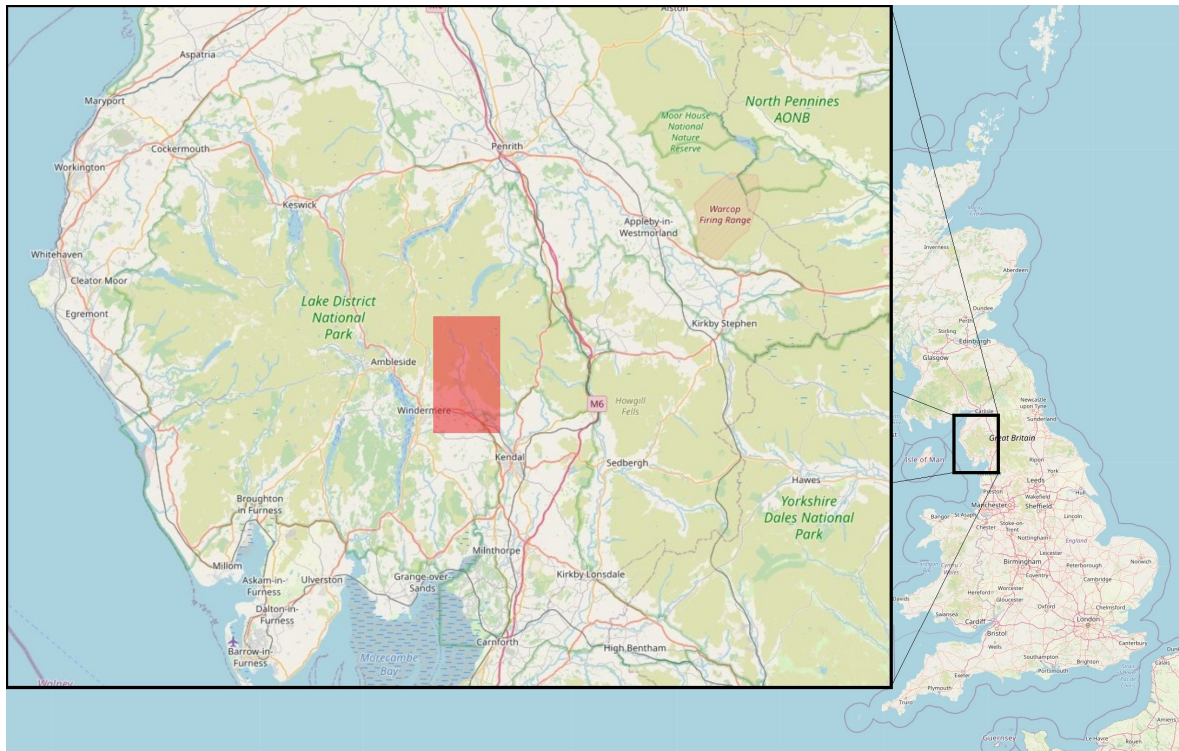


Figure 22: Catchment location, ©OpenStreetMap

4.1 Setup

Terrain and rainfall data was kindly provided by Barry Hankin. Additionally, elevation data was used from the National LIDAR Programme [12]. The network is modelled as 1764 river segments, with every segment containing a dam. However the dams are initially set to have $H^l = 100\text{m}$, meaning that under any realistic flow these dams will have no impact. A situation where $h \geq 100$ would certainly call for more drastic flood prevention measures. The network and its location is shown in Figure 23.

4.2 Rainfall Data

The rainfall data kindly provided by Barry gives inflows into each segment, generated using a dynamic topmodel [13]. The data represents inflow into each segment, not rainfall

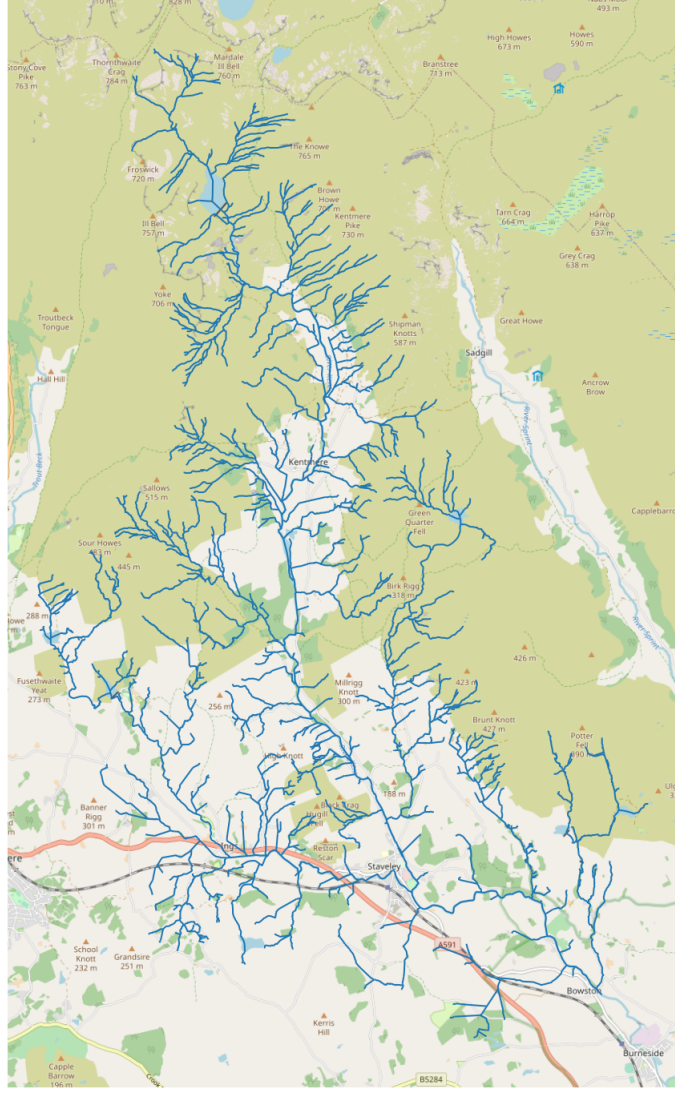


Figure 23: River Network

- so this includes considerations into groundwater flow and overland flow. To check the accuracy of my model I use data from the Bowston gauge, provided by NRFA ([10]).

To check the data, Figure 24 a) plots the total inflow into the whole network and the measures outflow at Bowston gauge, the final segment of the network. Note these represent different values - one is inflow into the whole network, the other is outflow at the lowermost segment. However, it's expected that these would give similar plots especially since the values are plotted over several months. However, it is clear that there is some discrepancy between the plots. Most notably, the total inflow is for long periods of time at $0\text{m}^3/\text{s}$ which is unrealistic - the river Kent doesn't just flow during storms. This is further reinforced by the large difference in the total volumes of water each flow predicts. From 1st Jan 2020 to 29th Feb 2020, the inflow data shows a total volume of $3.3 \times 10^7 \text{m}^3$, whereas the Bowston gauge records a volume of $5.3 \times 10^7 \text{m}^3$. To improve the accuracy of the data the difference is added as a baseflow, representing inflow from groundwater and stored water. This difference is proportioned over the river network according to the length ratios $\frac{l_i}{\sum_{j=1}^N l_j}$. This is shown in Figure 24 b).

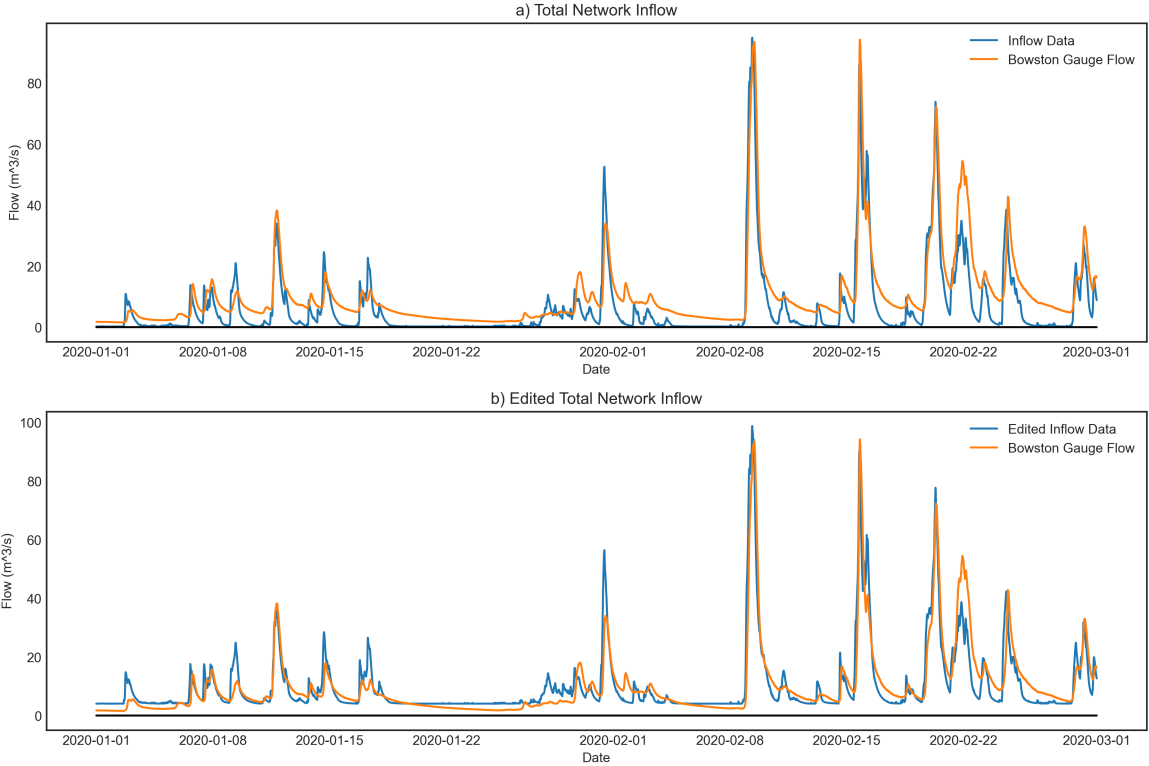


Figure 24: Plotting total network inflow and network outflow over time

4.3 Implementation

Both the numerical and hysteresis formulations are implemented in Python. Plots here will be from the numerical version due to its efficiency. The codes are presented with explanation and a worked through example in Jupyter notebooks on Github⁴. This also gives code on how to animate solutions so that the flow values over the whole network and details about the dam set-up can be visualised.

Additionally, as there are no segment widths given with the data, values have been calculated from the existing data. A list of segments which could potentially contain a leaky dam has been calculated, as these can only be built on sufficiently small streams. For the rest of this section I will focus on storm Ciara, the peak of which is around the 9th Feb 2020. λ is taken to be 20.

4.4 Results

Figure 25 shows some results for the network. Figure 25a) compares the predicted flow with the gauge readings. Plots b) to d) show effect of different numbers of identically build dams with properties $H^l = 0.3\text{m}$ and $H^u = 1.5\text{m}$. These dams are randomly placed on suitable branches of the network. For better visualisation, use the code in found in the GitHub repo⁵. From this, for all cases there is little impact on the maximum flow even if there is some impact on other areas. This is due to the dams all being created identically, and so it is likely that they have little impact on the peak of the flood (either by not being filled at all or by filling completely before the peak has arrived, see Section

⁴<https://github.com/robgondris/network-flood-model>

⁵<https://github.com/robgondris/network-flood-model>

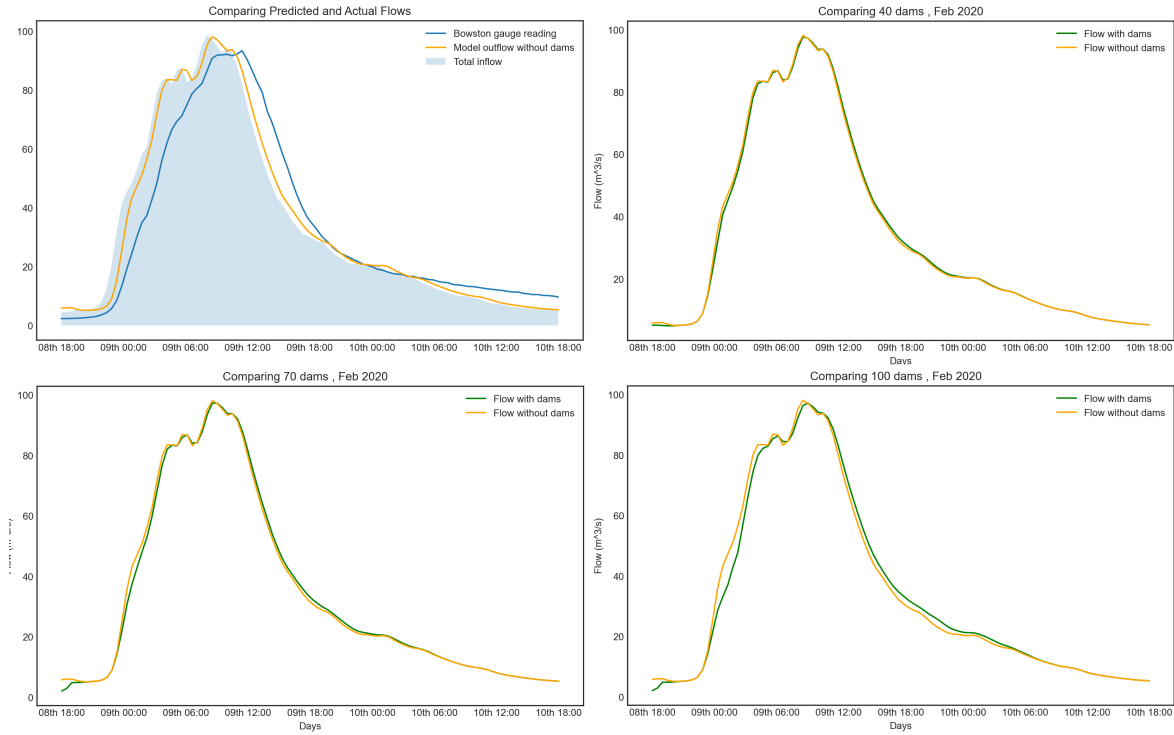


Figure 25: Uniform Dam Effectiveness

3.7). This can more clearly be seen in Figure 26, which plots how full each dam is as a percentage at a set time. There is a large range of problems - some have not had any impact at all, and others are completely full. This is animated in the GitHub code, the figure shows the state of the dams when the flow is maximal.

This is most clearly seen in Figure 25d), where the dams have an impact when the flow is still relatively low, and therefore a much smaller impact near the maximum flow.

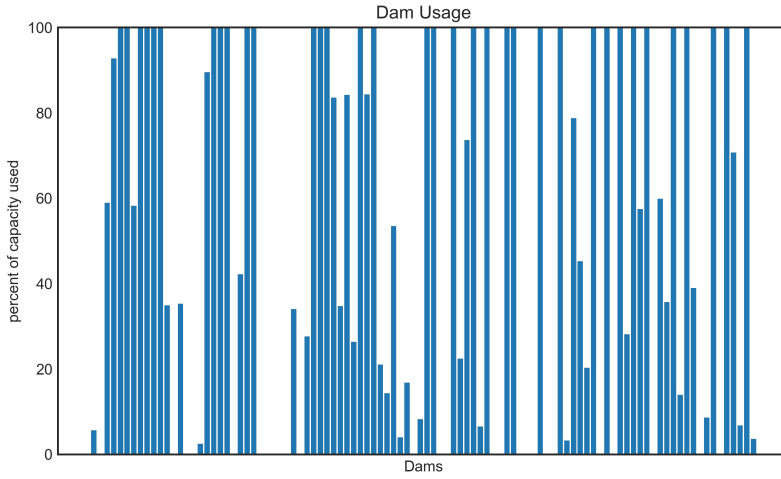


Figure 26: Dam capacity percentages at max flow for 25d)

This shows the need to design the dams in such a way that the majority of their impact is around the worst of the flood. One possible way of achieving this result is to first run a simulation with no dams, and for each segment calculate γ_i , the maximum height of the

river over the course of the flood. Then for each dam set $H_i^l = 0.85\gamma_i$. This will make sure the dams all have an impact when the flood is near its peak. The results are shown in Figure 27. Dam usage is shown in figure 28. Using 100 dams with this approach decreases the maximum flow by 3.7%, and for 200 dams there is a 5.9% decrease. This shows the value of designing the dams based on a model of the network with no dams. Also, the dams are used much more effectively, with almost all being used to their maximum capacity. However for this application an unreasonable number of leaky dams are required to have a significant effect. This goes without considering the additional cost of designing these specific dams.

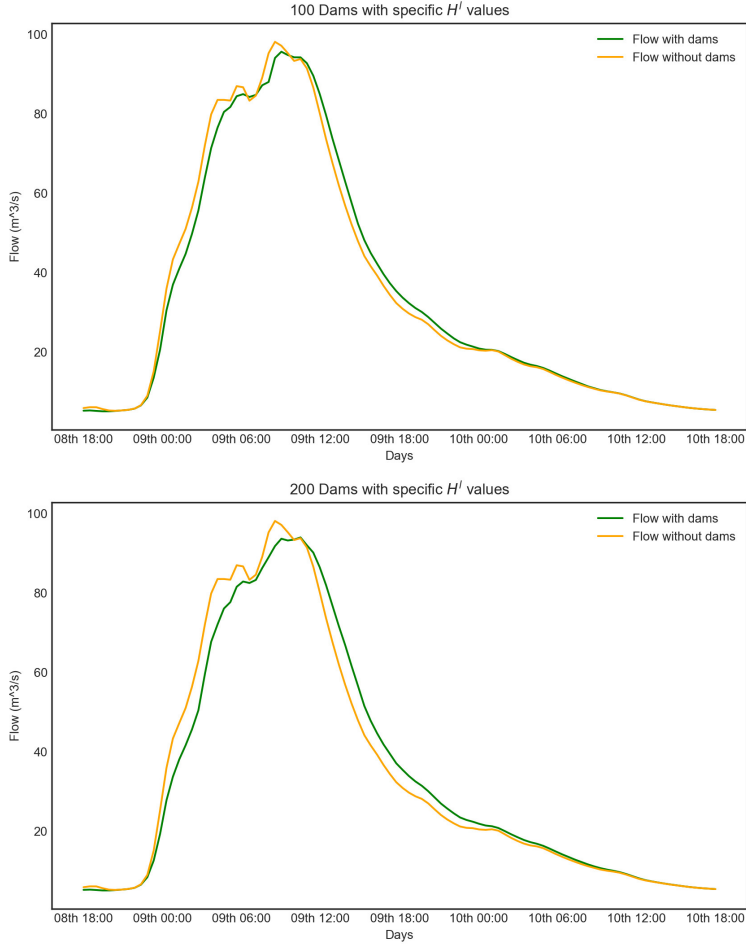


Figure 27: Dam Effectiveness where $H^l = 0.85\gamma$

If the dams have slightly different parameters, say $H_i^l = 0.5\gamma_i$, then there is a noticeable decrease in effectiveness as shown in 29. This could easily happen if the dams get partially blocked with debris, and as leaky dams wouldn't be maintained regularly. This is yet another difficulty that would need to be overcome.

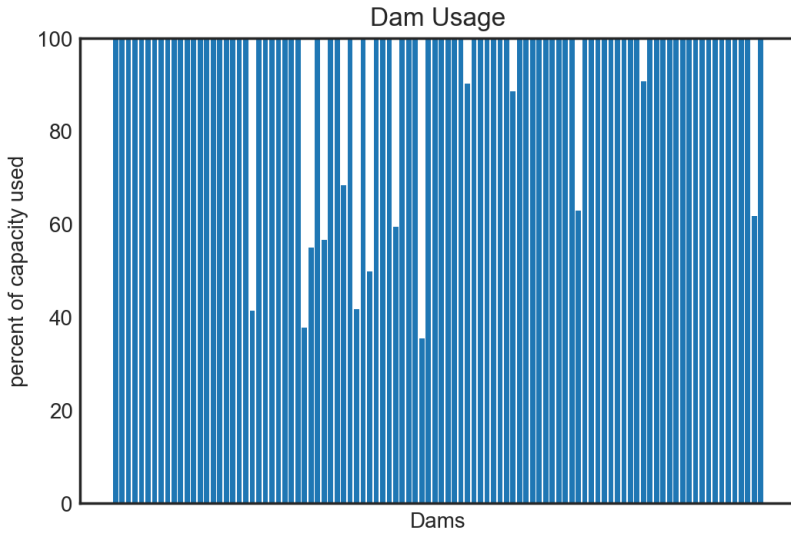


Figure 28: Dam capacity percentages at max flow for 27a))

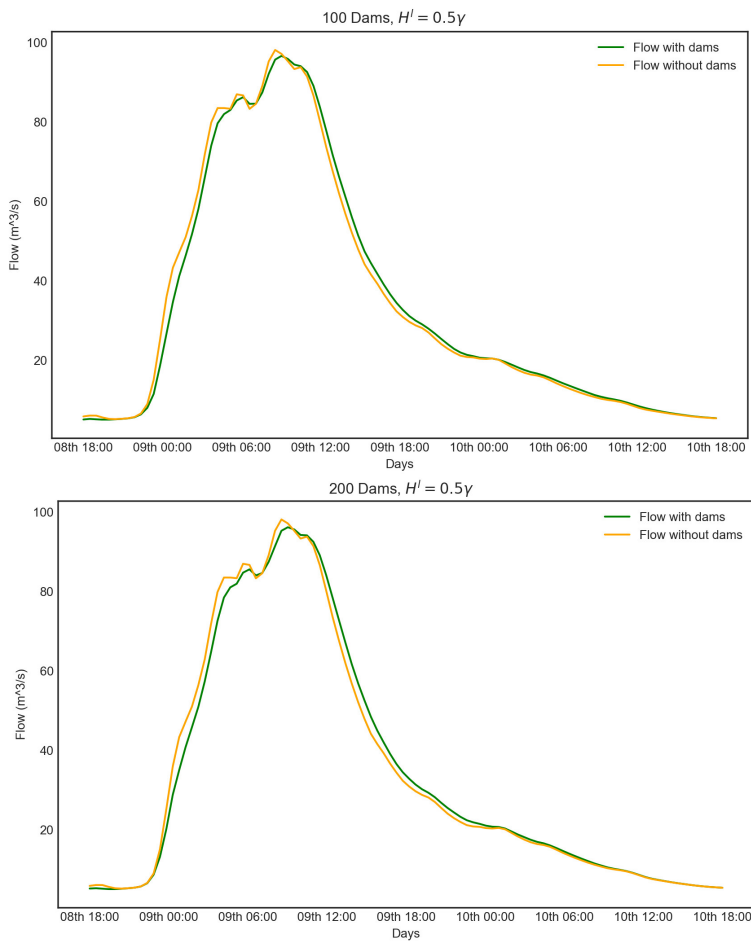


Figure 29: Dam Effectiveness where $H^l = 0.5\gamma$

These results are only for storm Ciara. When the dams are designed in this way, they will have different effects for different storms. Because the dams have been designed to start impacting when river heights reach 80% of Ciara's max height values, these dams

will have minimal impact for smaller storms.

This is a general problem - any dam set-up designed this way will impact a specific range of floods. This can be calculated with an analysis of expected peak flood values. As an example, the average yearly maximum flow value for Bowston is 64m^3 (NRFA [10]). A dam set-up can be constructed to impact floods of this height. However, this would only impact similar floods - it would have had minimal impact on the peak flow during storm Ciara for example. Having different dams to deal with different potential floods is a potential solution to this, but it would drastically increase the amount of dams that would have to be built.

4.5 Smaller Catchment

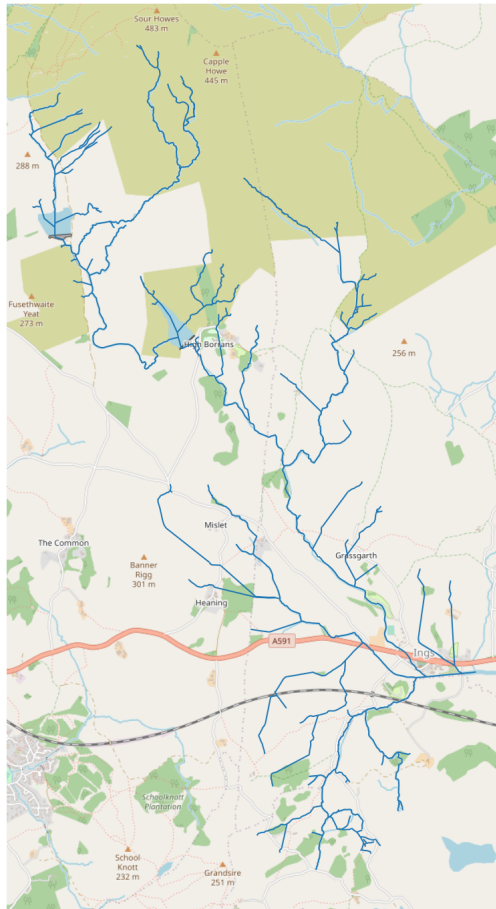


Figure 30: Smaller Network

In previous papers the catchment size has been much smaller, where the volume stored by dams is of a similar order to the total volume of inflowing water during a flood. This means that determining when a dam acts is far less important. To show this, a small subsection of the larger network is taken, shown in Figure 30. Plots for different dam set-ups are shown in Figures 31 and 32. Figure 31 compares uniformly constructed dams against designed dams. A uniform setup reduces maximum flow by 3.8%, whereas the designed dams reduce maximum flow by 4.7%. For small catchments it is most likely not be worth calculating exact dam specifications because uniformly constructed dams will still be effective.

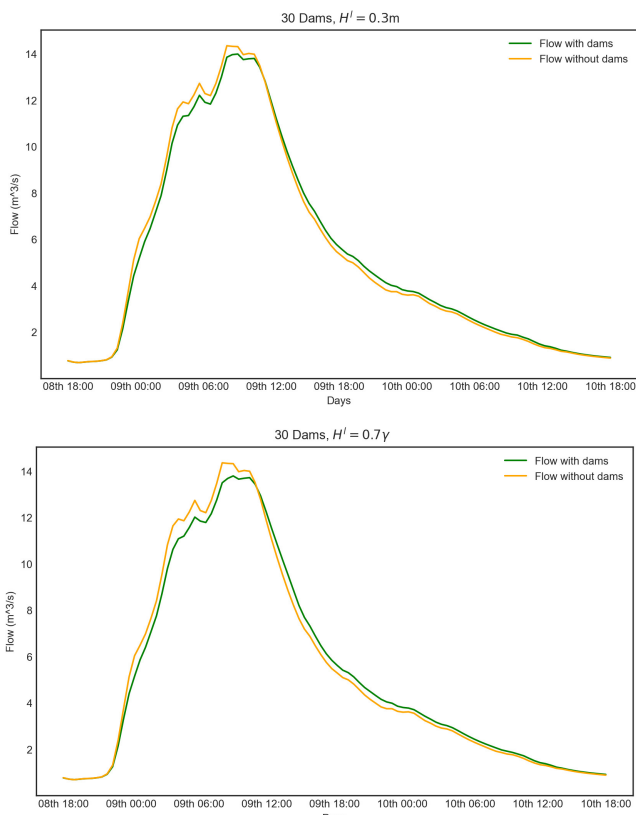


Figure 31: Comparing uniform dams to calculated dams

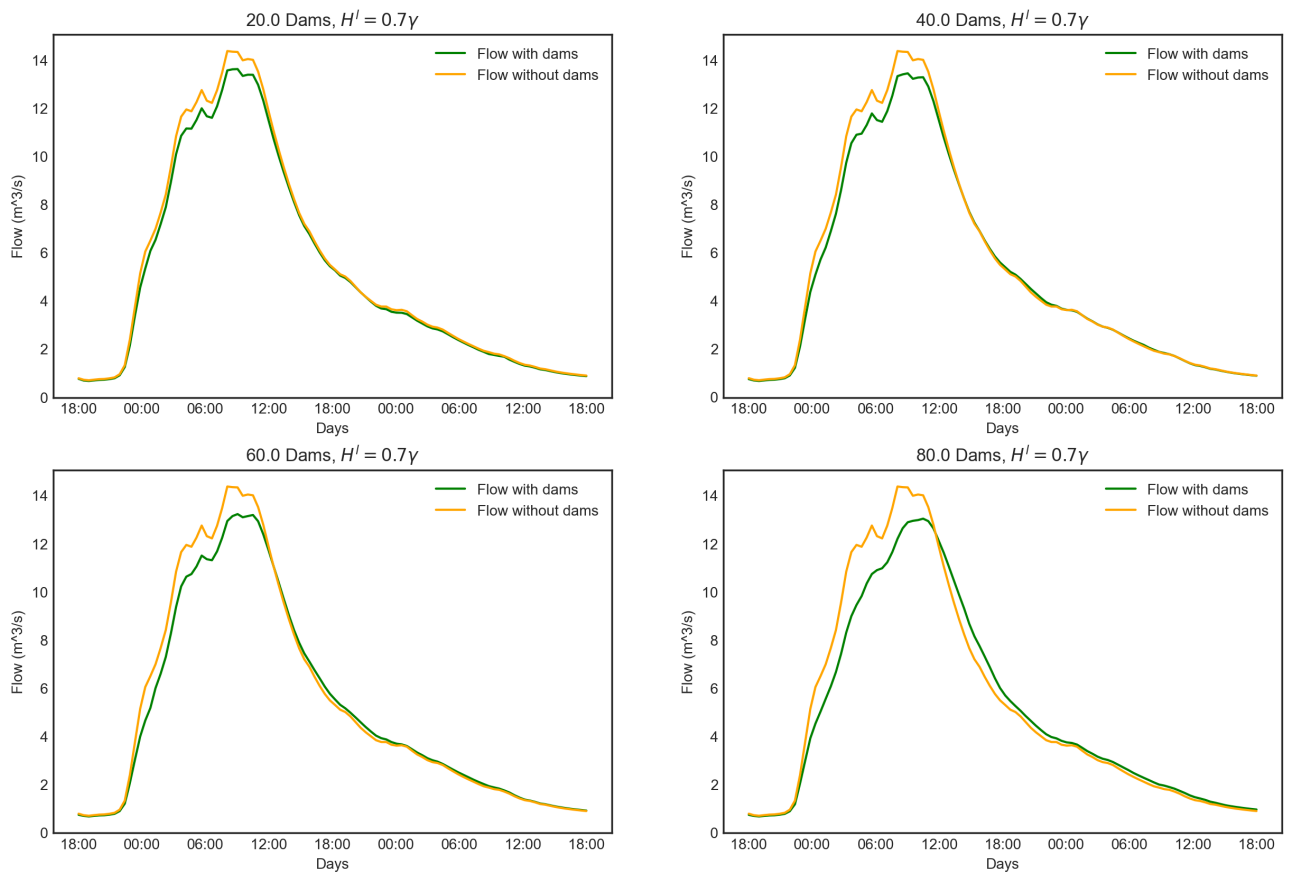


Figure 32: Comparing Number of Dams

Figure 32 compares how a different number of dams affect the flow. For 20, 40, 60 and 80 dams, the respective percentage decreases in max flow are 5.5, 6.9, 8.6 and 10.5%. This shows leaky dams can have a significant impact on smaller catchments.

5 Conclusion

In this project, I have derived a network based differential model for calculating the effect of leaky dams on river flow. I have written code that implements this, and a numerical approximation that is accurate and more efficient, which can be applied to any suitable network. I then apply this model to a network of 1764 segments, modelling a catchment of 71 km^2 , and a smaller section of this. I find that on a small network leaky dams are effective with random placement, although more effective placements can be found. However on a larger network simulations are necessary as a random placement of identical dams will likely have no effect on the maximum flow during a flood. Using the model dams can be constructed with parameters depending on their individual location, increasing their effectiveness significantly. However the amount of dams needed to have a meaningful impact is large, and I've also shown that small errors in the specifics of each dam leads to large decreases in effectiveness.

Overall leaky dams have the potential to be effective for larger catchments, however this requires a large number of them which are all built to specifications depending on their position in the river network.

6 Acknowledgements

This project was funded by an LMS Undergraduate Research Bursary and by Oxford University Mathematical Institute. I would like to thank my supervisor Prof. Ian Hewitt, whose help, insights and guidance were invaluable. I would also like to thank Barry Hankin and Rob Lamb from the JBA Trust who provided detailed data and many helpful suggestions.

References

- [1] Hankin B, Hewitt I, Sander G, Danieli F, Formetta G, Kamilova A, Kretzschmar A, Kiradjiev K, Wong C, Pegler S, Lamb R. *A risk-based, network analysis of distributed in-stream leaky barriers for flood risk management*. Natural Hazards and Earth System Sciences, in review (<https://www.nat-hazards-earth-syst-sci-discuss.net/nhess-2019-394/>)
- [2] Environment Agency (2020) *Working with natural processes to reduce flood risk* Available at: <https://www.gov.uk/government/publications/working-with-natural-processes-to-reduce-flood-risk> (Accessed: 1 September 2020)
- [3] Nicholson A, O'Donnell G, Wilkinson M, Quinn P *The potential of runoff attenuation features as a Natural Flood Management approach* J Flood Risk Management. 2020; 13 (Suppl. 1):e12565. <https://doi.org/10.1111/jfr3.12565>

- [4] HM Government (2018) *A Green Future: Our 25 Year Plan to Improve the Environment* Available at: https://assets.publishing.service.gov.uk/government/uploads/system/uploads/attachment_data/file/693158/25-year-environment-plan.pdf (Accessed: 1 September 2020)
- [5] Metcalfe P, Beven K, Hankin, B, Lamb R *Simplified representation of runoff attenuation features within analysis of the hydrological performance of a natural flood management scheme.* Hydrology and Earth System Sciences Discussions (<https://doi.org/10.5194/hess-2017-398>)
- [6] Munson R, Young D, Okiishi, T.H. (2006). *Fundamentals of fluid mechanics.* Hoboken, Nj: Wiley and Sons.
- [7] Chow, V., 1985. *Open-Channel Hydraulics.* Auckland: McGraw-Hill.
- [8] Hewitt I, (2019) *Mathematical Geoscience*, lecture notes, University of Oxford 2019 https://courses.maths.ox.ac.uk/node/view_material/39483 (Accessed 25 August 2020)
- [9] BBC News (2020) *Storm Ciara: Residents battle to save homes from floodwaters.* Available at: <https://www.bbc.co.uk/news/uk-england-cumbria-51433960> (Accessed: 1 September 2020)
- [10] Environment Agency (2020) *National River Flow Archive, Kent at Bowston* Available at: <https://nrfa.ceh.ac.uk/data/station/info/73017> (Accessed 1 September 2020)
- [11] SCRT, 2020 *Kendal Town View Fields – NFM project* Available at: <https://scrt.co.uk/what-we-do/current-projects/natural-flood-management/kendal-nfm-project> (Accessed 1 September 2020)
- [12] Environment Agency, 2020 *National LIDAR Programme* Used with an open government licence <http://www.nationalarchives.gov.uk/doc/open-governmentlicence/version/3/> Available at <https://data.gov.uk/dataset/f0db0249-f17b-4036-9e65-309148c97ce4/national-lidar-programme>
- [13] Metcalfe, Peter, Beven, Keith, Freer, Jim (2015). *Dynamic TOPMODEL: A new implementation in R and its sensitivity to time and space steps.* Environmental Modelling and Software. 72. 155-172. 10.1016/j.envsoft.2015.06.010.